Journal of Electroanalytical Chemistry 971 (2024) 118575

Contents lists available at ScienceDirect

Journal of Electroanalytical Chemistry

journal homepage: www.elsevier.com/locate/jelechem

Targeted microorganism detection with molecularly imprinted polymer biosensors

Hüseyin Oğuzhan Kaya [a], Yamaç Tekintaş [b], Fatma Kurul [c], Arif E. Cetin [c], Seda Nur Topkaya [a,*]

[a] Department of Analytical Chemistry, Faculty of Pharmacy, Izmir Katip Celebi University, Izmir, Turkey
[b] Department of Pharmaceutical Microbiology, Faculty of Pharmacy, Izmir Katip Celebi University, Izmir, Turkey
[c] Izmir Biomedicine and Genome Center, Izmir, Turkey

ARTICLE INFO

Keywords:
Molecularly imprinted polymers
Electrochemical biosensors
Bacteria detection
Antibiotic resistance
Electropolymerization

ABSTRACT

In this article, a molecularly imprinted polymer (MIP)-based electrochemical biosensor was developed for the detection of *Enterococcus faecium*, demonstrating exceptional selectivity and sensitivity in real urine samples. Our approach involved fabricating electrodes coated with bacteria-imprinted polypyrrole through electropolymerization. The surface characteristics of the molecularly imprinted polymer (MIP) and non-imprinted polymer (NIP) coated electrodes were thoroughly characterized using cyclic voltammetry and electrochemical impedance spectroscopy. Remarkably, the MIP-coated electrodes exhibited superior conductivity, highlighting their efficacy in capturing *Enterococcus faecium*. By subjecting the MIP-based biosensor to *Enterococcus faecium* incubation, we successfully monitored impedance changes, enabling the detection of minute quantities of the bacteria with a limit of detection of 9 CFU/mL. The technology could successfully distinguish *Enterococcus faecium* from *Enterococcus faecalis,* a related bacteria species within the same genus, marking a significant advancement in clinical differentiation. Additionally, the biosensor selectively captured *Enterococcus faecium* and discriminated it from other common bacteria, including *Proteus mirabilis, Escherichia coli, Staphylococcus aureus*, and *Pseudomonas aeruginosa.* This research underscores the utility of MIP-based electrochemical biosensors for the rapid and selective detection of *Enterococcus faecium* in clinical settings, with implications for targeted antibiotic therapy and infection control.

1. Introduction

The genus Enterococcus comprises bacteria that appear as individual, paired, or short chains of gram-positive cocci. *Enterococcus faecium* and *Enterococcus faecalis* are common bacteria associated with enterococcal infections and are found in the microbiota of both animals and humans. These bacterial strains have the capacity to cause a variety of infections, such as urinary tract infections, wound infections, endocarditis, and bacteremia, underscoring their clinical importance in healthcare settings [1]. They can be found in diverse sources, such as food, plants, water, and soil. *E. faecium* demonstrates the remarkable ability to thrive and endure in a wide range of extreme environmental conditions. It is frequently transmitted through high-contact surfaces such as alarm buttons, door handles, bed surfaces, toilet seats, and blood pressure monitors. In recent years, *E. faecium* has emerged as a major contributor to nosocomial infections, demonstrating higher levels of antibiotic resistance and mortality rates compared to *E. faecalis*. It exhibits resistance to multiple antibiotics, including ampicillin and vancomycin, significantly limiting the available treatment options for infections caused by these bacteria. As bacteria evolve and develop resistance mechanisms against antibiotics, commonly used treatments become less effective, leading to prolonged illnesses, increased healthcare costs, and, in severe cases, mortality. Furthermore, distinguishing between *E. faecalis* and *E. faecium* is crucial because antibiotics effective against *E. faecalis* may not work for *E. faecium*. This means that the treatment approach for each bacterium needs to be carefully tailored, as the same antibiotics cannot be used interchangeably [2].

Various detection technologies are available for identifying bacteria, which are broadly categorized into methods targeting either the whole microorganism or its metabolites. These include general approaches such as microscopy and culture-based techniques, as well as specific assays like biochemical tests, Polymerase Chain Reaction (PCR) [3], DNA sequencing [4], Fluorescence in situ Hybridization (FISH) [5], Enzyme-Linked Immunosorbent Assay (ELISA) [6], Matrix-Assisted

* Corresponding author.
E-mail address: sedanur.topkaya@ikcu.edu.tr (S. Nur Topkaya).

https://doi.org/10.1016/j.jelechem.2024.118575
Received 7 June 2024; Received in revised form 29 July 2024; Accepted 13 August 2024
Available online 21 August 2024

Laser Desorption/Ionization Time-of-Flight Mass Spectrometry (MALDI-TOF) [7], and Next-Generation Sequencing (NGS) [8]. The choice depends on factors such as bacterial species, sensitivity, specificity, resources, and application, often involving a combination of methods to leverage their respective strengths and address limitations. Microscopy offers morphological insights, while culture-based methods enable identification and sensitivity testing. Biochemical assays aid in bacterial characterization. Molecular methods like PCR and DNA sequencing provide high specificity. ELISA is suitable for screening. MALDI-TOF and NGS offer rapid and comprehensive detection but require costly equipment and specialized expertise.

Biosensor methodologies could be promising for detecting pathogens in various media such as blood, serum, urine, food, and water, with minimal sample pre-treatment, simplifying detection processes [9]. Electrochemical-based biosensors are preferred for bacteria detection due to their sensitivity, speed, specificity, cost-effectiveness, and real-time monitoring. They require minimal samples, making them ideal for early diagnosis and point-of-care testing. Their compact design allows easy integration into portable devices, enhancing accessibility in remote locations and field conditions. In electrochemical biosensors, Molecularly Imprinted Polymers (MIP) play a pivotal role, establishing a crucial link between selective molecular recognition and efficient detection [10,11]. These synthetic polymeric structures have binding sites tailored for target molecules such as bacteria or proteins. In electrochemical biosensors, MIPs act as recognition elements, capturing targets with exceptional selectivity and altering electrical properties, which the electrode measures. Integrating MIPs with electrochemical platforms creates robust, efficient biosensors capable of detecting various analytes. A key benefit of MIPs is their ability to be direct engineering onto the electrode surface [12].

MIPs offer a low-cost, scalable alternative to biological receptors, with exceptional selectivity and durability. They can bind specific target molecules in complex mixtures and withstand harsh conditions. However, MIPs face challenges such as the complex, time-consuming optimization of the monomer-template ratio and the lengthy process of template extraction from the polymer matrix [13]. MIP synthesis involves selecting a template molecule for specific recognition, choosing functional monomers for strong interactions, and polymerizing the mixture with a free radical initiator and cross-linker to form a stable network. The template is then removed, leaving cavities that specifically bind the template molecule. This process creates a polymer with custom-imprinted cavities, which alter the electrode surface's electron transfer properties, monitored using voltammetric and impedimetric techniques. Among the types of polymers used in the literature, pyrrole is one of the most suitable for creating an MIP structure to detect analytes with various molecular weights. This is because the transformation of pyrrole into polypyrrole through electropolymerization has been widely performed, and electropolymerization can be well-controlled, making the final structure more predictable [14]. Additionally, the biocompatibility of the polypyrrole structure with bone marrow, immune system cells of the mammary glands, etc., increases its usability [15]. Non-imprinted polymers (NIPs), synthesized similarly to MIPs but without a template, form non-specific cavities, which can lead to leading to non-specific binding. NIPs serve as controls to evaluate the selectivity and specificity of MIPs. [16]. NIP lack the specific molecular recognition sites of MIP, featuring a homogeneous polymer matrix that does not selectively bind molecules. This makes NIP valuable as control samples for comparing non-specific to specific binding effects of MIP.

In this study, we developed an MIP-based electrochemical biosensor for detecting *E. faecium* bacteria. This biosensor uniquely combines the specificity of MIP with the sensitivity of electrochemical detection to selectively identify *E. faecium* in complex biological samples, including real urine. One critical aspect of biosensor selectivity is the ability to discriminate among similar structures. Using our biosensor, *E. faecium* has been successfully distinguished from *E. faecalis* for the first time, marking a significant achievement in sorting these closely related bacteria in clinical settings using rapid electrochemical techniques. This differentiation, despite minimal structural differences, represents a notable advancement, particularly in the context of varying antibiotic resistances observed between these two bacteria. Furthermore, we selectively captured *E. faecium* using the MIP structure and distinguished it from *Proteus mirabilis, Escherichia coli, Staphylococcus aureus,* and *Pseudomonas aeruginosa.* Our study represents the first documented instance of such differentiation in the literature for these bacteria. Our results also highlight the biosensor's potential to address the challenge of antibiotic resistance by ensuring appropriate antibiotic usage based on precise pathogen identification. Another significant discovery from our study was that *E. faecium's* conductivity significantly enhances the polymerization of pyrrole and its deposition onto electrodes, demonstrating the potential for the development of conductive surfaces using a variety of materials. We also showed that our biosensor platform supports a lower limit of detection (LOD) compared to the literature for *E. faecium* in artificial and real urine samples. This biosensor consistently detects bacteria in real samples and its adaptable MIP-based platform suggests it could be a scalable tool for broader infectious disease management, setting a new standard in rapid bacterial pathogen detection.

2. Materials and methods

2.1. Chemicals, apparatus and instruments

The chemicals used in the experiment were supplied from various manufacturers. PBS tablets were purchased from BioShop, and pyrrole, creatinine and albumin were obtained from Sigma-Aldrich. Sodium hydroxide (NaOH), sodium chloride (NaCl), potassium dihydrogen phosphate (KH_2PO_4), potassium hexacyanoferrate(II) trihydrate ($K_3[Fe(CN)_6]$), and potassium hexacyanoferrate(III) ($K_4[Fe(CN)_6]$), Glycerin Brain Heart Infusion medium, and Tryptic Soy Agar (TSA) were supplied by Merck.

Sodium dodecyl sulfate (SDS) was purchased from Serva, potassium chloride (KCl) from Panreac, absolute ethanol (99.9 %) and glacial acetic acid from Isolab Chemicals, and sodium phosphate from Roth and Amresco. Buffers used included 0.5 M acetate buffer (ACB, pH 4.8) and 0.05 M phosphate buffer (PBS, pH 7.4). All solutions were prepared with ultrapure water (UPW).

Pencil graphite electrodes (PGEs) were used as the working electrodes, with a platinum wire serving as the auxiliary electrode and an Ag/AgCl reference electrode. Pencil leads (0.5 mm) with grade of HB manufactured by Tombow, Japan, were purchased from a local book store. The 10 mm graphite leads were immersed for both measurement and immobilization steps. Pencil Model T 0.5 mm (Rotring, Germany), was used as a holder for pencil lead. Electrochemical measurements were performed using an AUTOLAB 204.FRA32M with NOVA 2.1 software. A Carl Zeiss 300VP SEM was used to image PGE surfaces, bacteria, and MIP formations. Samples were gold-coated using a Quorum Q150 Res before SEM analysis. DLAB MX-S was used for vortexing, and the Biosan McFarland DEN-1B served as the densitometer.

2.2. Bacteria

Bacteria were isolated during routine clinical procedures at Izmir Katip Celebi University Medical Faculty Hospital and identified using MALDI-TOF MS (Bruker Daltonics, Bremen, Germany). A fresh culture was prepared by transferring a 10 μL sample from the stock stored at −80 °C onto TSA. After 18 h of incubation at 37 °C, colonies were transferred to tubes, homogenized at 400 rpm for 30 s, and the concentration was determined to be 10^8 CFU/mL using densitometry.

2.3. Preparation of artificial and real urine samples

The artificial urine samples were prepared using the following formulation: albumin (50 mg/L), creatinine (2 g/L), urea (18.2 g/L),

sodium chloride (7.5 g/L), sodium phosphate (4.8 g/L) and, potassium chloride (4.5 g/L). The pH was adjusted to 5.1. Real urine specimens were collected from healthy volunteers. *E. faecium* was prepared with PBS for a concentration range from 10^2 to 10^8 CFU/mL. The bacterial samples were then diluted to the desired concentrations.

2.4. Preparation of molecularly imprinted polymer (MIP) and Non-Imprinted polymer (NIP)

The graphite electrodes were activated by immersing them in a solution of ACB and applying a potential of +1.4 V for 30 s. Subsequently, the electrodes were immersed in a 0.1 M KCl solution containing 10^7 CFU/mL *E. faecium* and 50 mM pyrrole [17]. The electrodes underwent electropolymerization with a scan rate of 75 mV/s for 7 cycles in the potential range of 0 to +0.95 V. This process resulted in the coating of the electrodes with bacteria and polypyrrole [18]. Following this, *E. faecium* was removed from the polymer surface by treating it with a solution containing 10 % (v/v) acetic acid and 10 % (w/v) SDS for 2 h [19]. This process allowed for the synthesis of the MIP structure, while the NIP structure was prepared using a 0.1 M KCl solution with 50 mM pyrrole monomer in the absence of *E. faecium,* under the same electropolymerization conditions. After the formation of *E. faecium*-specific cavities on the MIP surface, the electrodes were subjected to *E. faecium* solutions of different concentrations prepared in PBS, and placed in a thermal shaker. The same experimental conditions were applied to the NIP structures as control group. Stirring was carried out at 400 rpm for 1 h at 25 °C. Following incubation, the electrodes were washed once with PBS to remove any bacteria not adhering to the surface.

2.5. Measurement

Cyclic Voltammetry (CV) was performed between −0.05 V and +0.6 V at 50 mV/s in 10 mM $K_3/_4[Fe(CN)_6]$. Electrochemical Impedance Spectroscopy (EIS) was conducted between 10^5 Hz and 10^{-1} Hz with a 0.01 amplitude and 10 frequencies per decade.

3. Results and discussion

3.1. Step-by-step sensor fabrication

Determining the suitable functional monomer for the synthesis of selective recognition units depends on multiple parameters, including the degree of polymerization, the electropolymerization's potential window, and the functional moieties inherent in the designated polymer [20]. When a potential is applied, monomers undergo electrochemical oxidation, generating radicals that initiate polymerization, forming a polymeric film on the working electrode's surface. This film can be conductive or non-conductive, depending on the monomers and polymerization conditions [21]. In our study, the polymerization of pyrrole monomer into polypyrrole was conducted, and the optimal conditions for polymerization were established before forming the MIP structure. Polypyrrole was synthesized on the electrode surface through electropolymerization (Fig. 1A).

Fig. 1B shows the impact of the number of cycles on polypyrrole electropolymerization using CV. Deposition was achieved by applying a potential of 0 to +0.95 V in 0.1 M KCl with 50 mM pyrrole. After electropolymerization, the associated redox currents were measured.

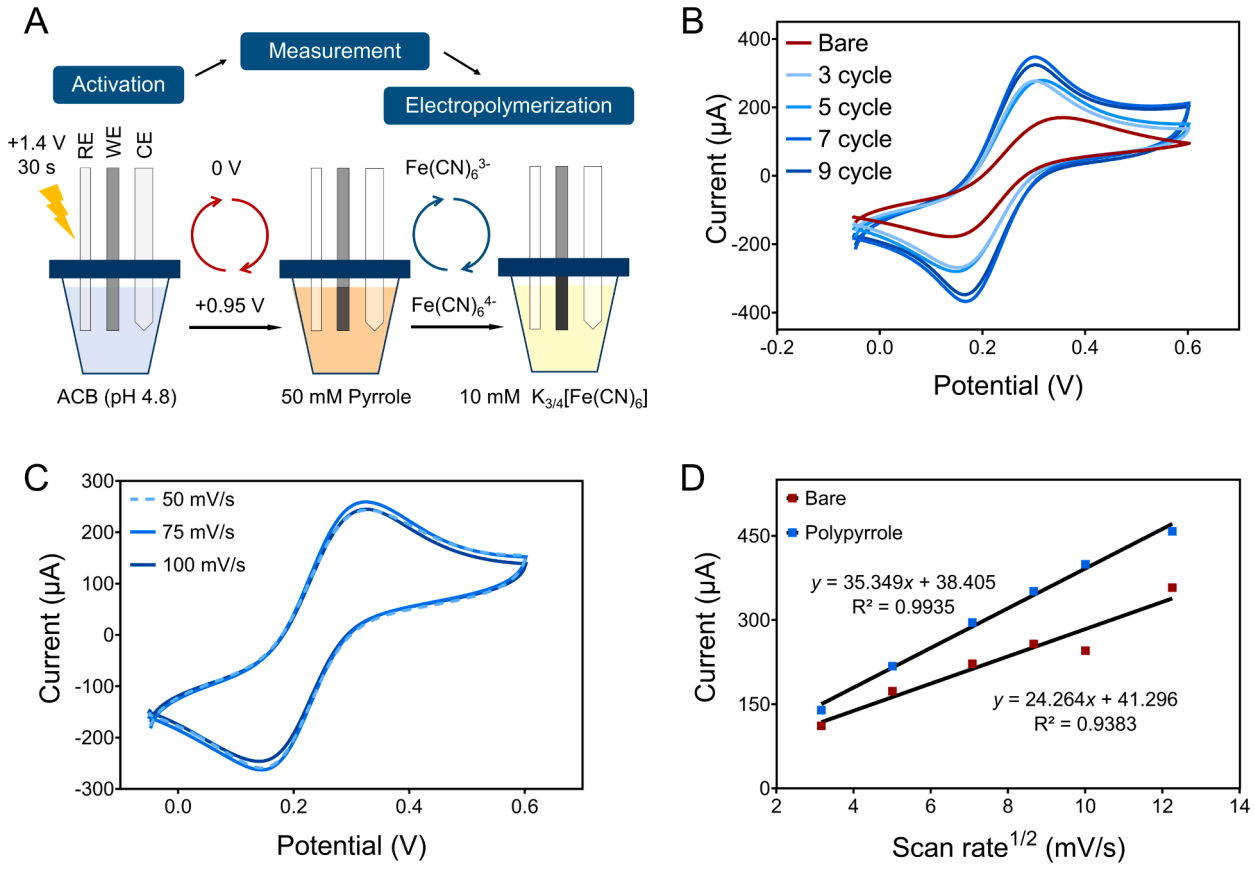

Fig. 1. **(A)** Experimental conditions for polymerization of pyrole monomer. **(B)** CV curves of the bare and polypyrrole-coated electrodes prepared with 3, 5, 7, and 9 cycles in 50 mM pyrrole, measured in 10 mM $K_3/_4[Fe(CN)_6]$ solution in the potential range of −0.05 V to +0.6 V. **(C)** CV curves of polypyrrole-coated electrodes prepared with 7 cycles in 50 mM pyrrole, measured in 10 mM $K_3/_4[Fe(CN)_6]$ solution at the scan rates of 50, 75, and 100 mV/s in the potential range of −0.05 V to +0.6 V. **(D)** The relationship between the square root of the scan rate and the oxidation currents of $K_3/_4[Fe(CN)_6]$ solution obtained from CV at various scanning rates for the bare and polypyrrole-coated electrodes.

Polypyrrole electropolymerization increased redox currents, with optimal conductivity achieved at 7 coating cycles. Beyond this point, no further improvement was observed, indicating surface saturation. Thus, 7 cycles were used for subsequent experiments.

The influence of the scan rate on the electropolymerization process was investigated at rates of 50, 75, and 100 mV/s. As shown in Fig. 1C, the optimal polypyrrole coating on the electrode surface, resulting in the highest oxidation currents in the 10 mM $K_3/_4[Fe(CN)_6]$ solution, was achieved at a scan rate of 75 mV/s, where the maximum conductivity, corresponding to the maximum polypyrrole coating, was attained.

After coating, the conductivity and electroactive surface areas of polypyrrole-coated and bare electrodes were evaluated. CV measurements were performed at the scanning rates ranging from 10 to 150 mV/s, including 10, 25, 50, 75, 100, and 150 mV/s in 10 mM $K_3/_4[Fe(CN)_6]$ solution. Fig. 1D shows that polypyrrole-coated electrodes exhibit higher redox currents than bare electrodes, with currents increasing with the scan rate. The active surface areas of the polypyrrole-coated and bare electrodes were determined using the Randless-Sevcik equation, which considers the measured currents and scan rate values:

$$i_p = 2.69 \times 10^5 \sqrt{SD}\sqrt{n^3}C\sqrt{v} \quad (1)$$

where S is the surface area (cm^2), D is the diffusion coefficient (7.66×10^{-6} cm^2/s for $[Fe(CN)_6]^{3/4-}$), n is the number of transferred electrons ($n = 1$), and C is the total concentration of electroactive species (mol/cm^3).

According to Eq. (1), the surface area of the polypyrrole-coated

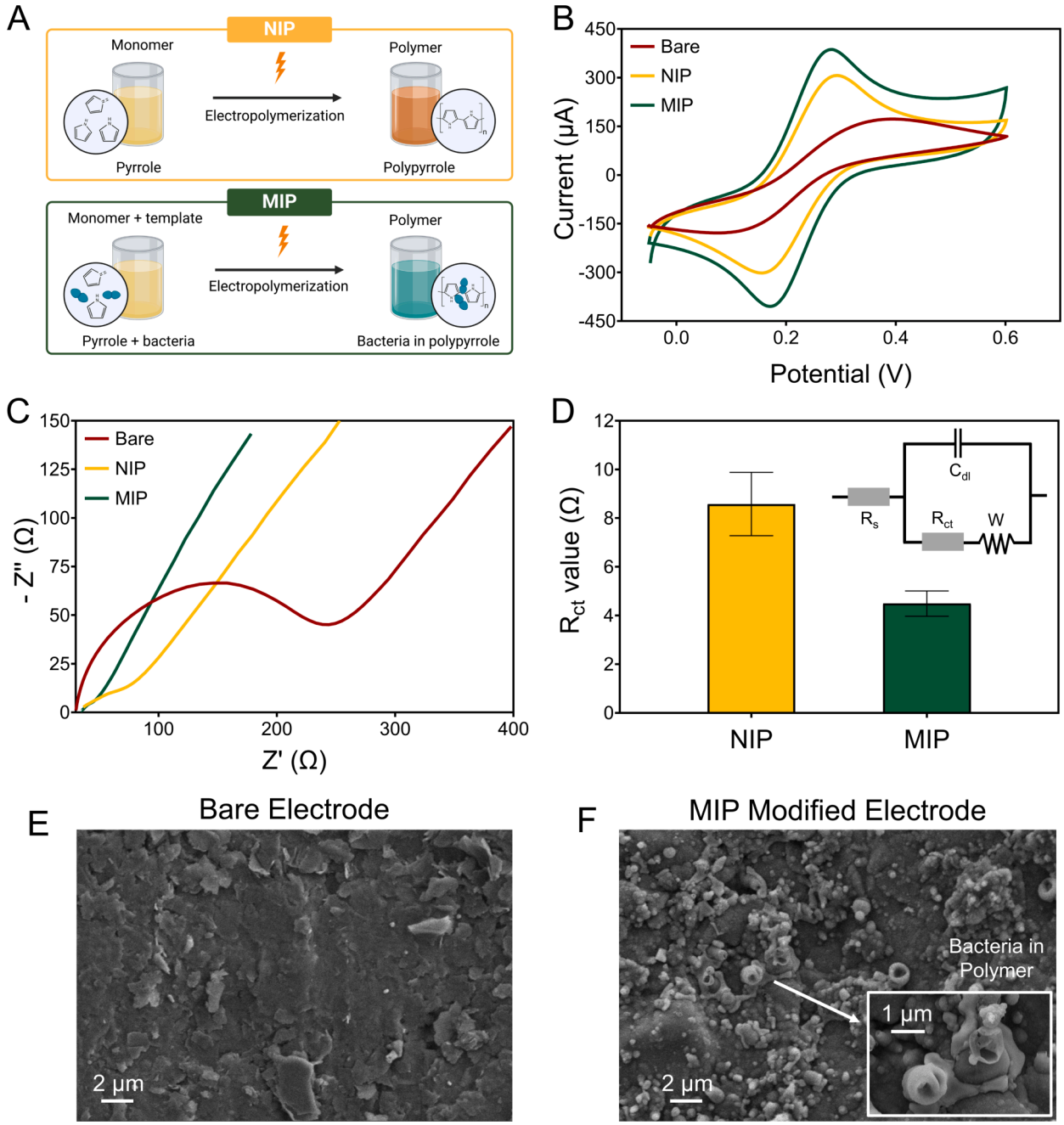

Fig. 2. **(A)** Formation of NIP and MIP structures. **(B)** CV and **(C)** EIS responses for bare, NIP- and MIP-modified electrodes measured in 10 mM $K_3/_4[Fe(CN)_6]$ solution. **(D)** The average R_{ct} values resulting from EIS measurements of MIP- and NIP-modified electrodes in 10 mM $K_3/_4[Fe(CN)_6]$ solution. SEM images of **(E)** bare and **(F)** MIP-modified electrodes.

electrode was 18.1 mm^2, compared to 12.2 mm^2 for the bare electrode, indicating a 48 % increase. This increase in electroactive surface area explains the higher oxidation currents observed at polypyrrole-coated electrodes due to enhanced conductivity. Similar to other polypyrrole modifications reported in the literature, our sensor shows a significant improvement in both conductivity and electroactive surface area [22]. For example, in the study conducted by Kilic et al., the surface area of screen-printed electrodes coated with polypyrrole was found to be 16.6 mm^2, while the surface area of the plain screen-printed electrodes was 10.2 mm^2 [23]. In another study, glassy carbon electrodes coated with

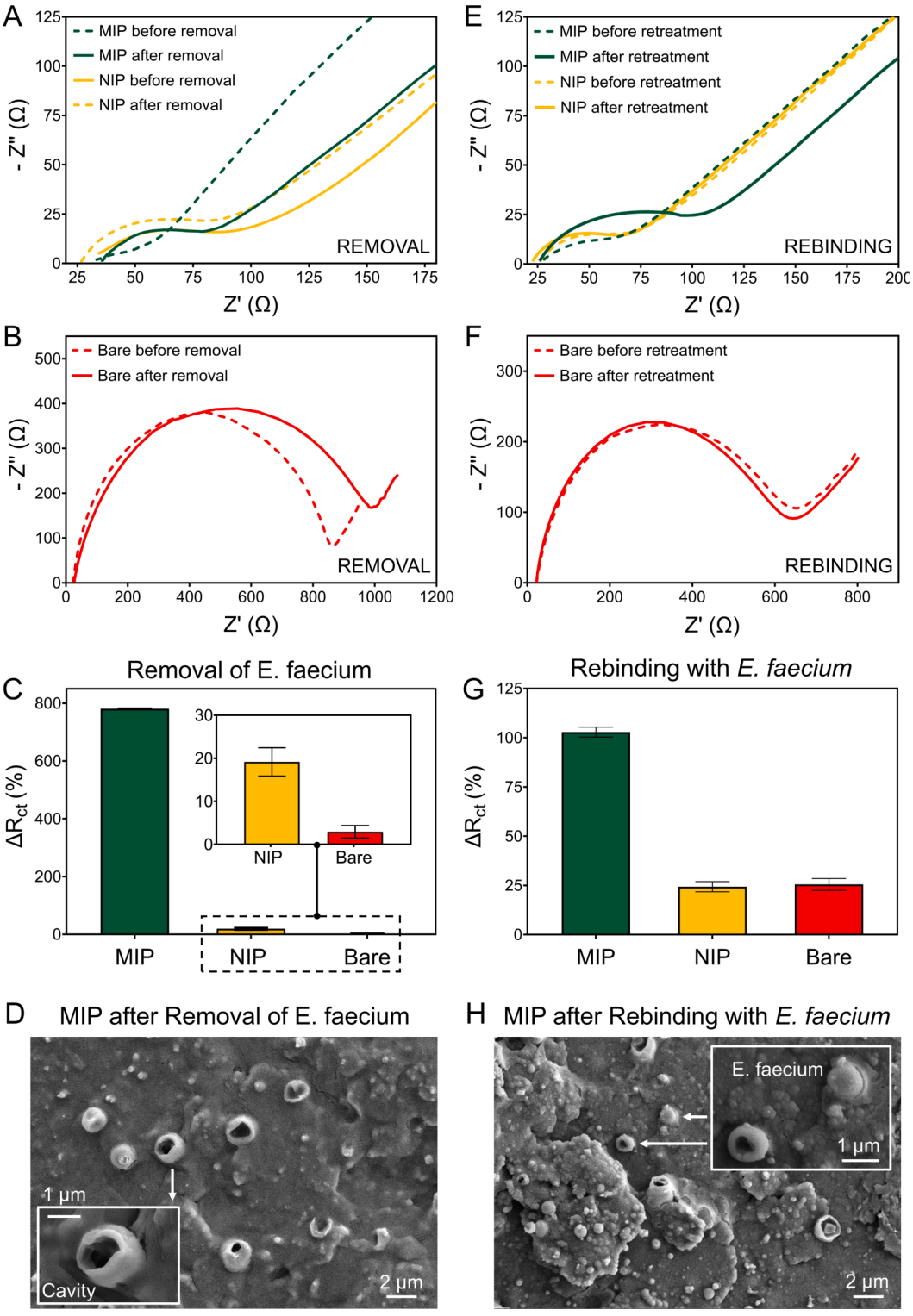

Fig. 3. EIS response for **(A)** MIP, NIP modified and **(B)** bare electrodes measured in 10 mM $K_3/_4[Fe(CN)_6]$ solution before and after treatment with a removal agent. **(C)** ΔR_{ct} values before and after the treatment of MIP, NIP, and bare electrodes with the removal agent. **(D)** SEM image of the MIP after the removal of *E. faecium*. EIS response for MIP, NIP modified **(E)** and bare **(F)** electrodes before and after retreatment with *E. faecium*. **(G)** The graph illustrates ΔR_{ct} determined by EIS conducted in a 10 mM $K_3/_4[Fe(CN)_6]$ solution before and after retreatment of MIP, NIP, and bare electrodes with *E. faecium*. **(H)** SEM image of the MIP after the rebinding with *E. faecium*.

polypyrrole exhibited an electroactive surface area of 12.5 mm^2 [24].

Bacteria-imprinted polymers were prepared under the optimized electropolymerization conditions for polypyrrole coating (Fig. 2A). A 0.1 M KCl solution containing 50 mM pyrrole and 10^7 CFU/mL *E. faecium* was used for the electropolymerization of bacteria-imprinted polypyrrole. NIP was prepared without adding a template molecule to assess whether the developed MIP structure contains specific cavities for the target analyte serving as a control against MIP.

Fig. 2B shows CV results for bare, MIP-modified, and NIP-modified electrodes. MIP-modified electrodes with *E. faecium* exhibited higher redox currents than bare and NIP-modified electrodes, indicating template bacteria attachment and increased conductivity [25]. This phenomenon is attributed to electrostatic repulsion between bacteria and redox probes. However, *E. faecium* enhances pyrrole polymerization and deposition, which deviates from existing literature, suggesting potential applications in creating conductive surfaces with nanomaterials and polymers.

EIS results (Fig. 2C) exhibit similar differences between bare, MIP-modified, and NIP-modified electrodes, supporting our CV findings. The impedimetric MIP-based electrochemical biosensor measures the changes in the film impedance or capacitance across a range of frequencies. The half-rotating impedance diameter equating to the charge-transfer resistance (R_{ct}) of the bare electrodes (154 ± 24 Ω) is much higher than that of the MIP- (4.5 ± 0.5 Ω), and NIP-modified (8.6 ± 1.3 Ω) electrodes, i.e., the data regarding the bare electrodes were not included in Fig. 2D. R_{ct} of the MIP-modified electrodes was 51 % lower than that of the NIP-modified electrodes. This suggests that bacteria contribute to the conductivity during MIP formation, and become incorporated into the polymer structure on the electrode surface alongside pyrrole.

As noted in the literature, using a polypyrrole structure has allowed the whole bacterial cell (*E. faecium* in our study) to be incorporated into the MIP structure [15]. These results are consistent with the CV data. Fig. 2E and 2F show the SEM images of bare and MIP-modified electrodes, respectively.

To create *E. faecium*-specific cavities in the MIP structure, *E. faecium* used during electropolymerization was removed. The challenge with imprinting bacteria is their size, complicating cell removal from template cavities. In this study, 10 % acetic acid with 10 % SDS was used as the removal agent. Even at 0.5 %, acetic acid harms most bacteria by lowering intracellular pH and disrupting metabolic processes. Stirring was intentionally avoided during this process to prevent any potential damage to the polymer structure on the electrode surface, ensuring its integrity for subsequent studies. In our study, the bare, MIP- and NIP-modified electrodes were treated with the removal solution for 2 h. To evaluate the influence of the removal solution, bare, MIP- and NIP-modified electrodes were also subjected to a treatment with water as a control study. Fig. 3A shows the EIS spectra before (dashed curves) and after (solid curves) the removal of *E. faecium* for the MIP- (green curves) and NIP-modified (yellow curves) electrodes. Fig. 3B shows the EIS spectra before (dashed red curves) and after (solid red curves) the removal of *E. faecium* for the bare electrodes. ΔR_{ct} was calculated by subtracting the R_{ct} value of the electrodes treated with the removal agent from the R_{ct} value of those treated with water.

Fig. 3C shows the percentage change within the ΔR_{ct} determined from the EIS response before the removal from that of after the removal for the MIP- (green) and NIP-modified (yellow), and bare electrodes (red), where the error bars correspond to the SD values of five independent experiments, using the formula below:

$$\Delta R_{ct}(\%) = 100 \times \frac{R_{ct}(Beforeremoval) - R_{ct}(WaterTreatment)}{R_{ct}(Afterremoval) - R_{ct}(WaterTreatment)}$$

As shown in Fig. 3C, R_{ct} of MIP-modified electrodes after the treatment with the removal solution dramatically increased, e.g., the removal of *E. faecium* from the polymer surface, resulting in a ~8-fold (~800 % in the figure) increase in the ΔR_{ct} of the MIP-modified electrodes compared to the ΔR_{ct} of the electrode before the removal. The NIP layer was formed similarly to MIP, e.g., only bacteria were not added, and the abovementioned extraction solutions similarly treated the NIP-modified electrodes. The ΔR_{ct} of the NIP-modified electrodes increased after the treatment with the removal solution by only ~20 %, which could be neglectable in the presence of the impedance variations observed for MIP-modified electrodes. In another study in which dibutyl phthalate was detected with a molecularly imprinted polymer-based sensor using polypyrrole, the biggest change in impedance measurements after the removal of the mold molecule dibutyl phthalate from the structure occurred with the removal of the mold molecule in MIP-coated electrodes, similar to our study, while the impedance value of NIP-coated electrodes increased slightly with the effect of the removal agent, but this increase was very limited compared to MIP modified electrodes [26]. On the other hand, bare electrodes remained almost stable before and after the treatment with the removal agents. Fig. 3D shows the SEM image of the MIP after the removal of *E. faecium*.

To assess the efficacy of MIP-modified electrodes' efficacy in detecting *E. faecium,* MIP-, NIP-modified, and bare electrodes were exposed to *E. faecium* at 10^6 CFU/mL. Fig. 3E shows EIS spectra before (dashed) and after (solid) *E. faecium* rebinding for MIP- (green) and NIP-modified (yellow) electrodes. Fig. 3F shows EIS spectra for bare electrodes (red). Fig. 3G shows the ΔR_{ct} percentage change before and after rebinding for MIP-, NIP-modified, and bare electrodes, with error bars indicating SD values from five experiments. MIP-modified electrodes exhibited approximately a 100 % increase in ΔR_{ct} increase, attributed to bacteria coating specific MIP cavities which impedes electron transfer and increasing film impedance. In the absence of bacteria-specific cavities on the surface of the NIP-modified and bare electrodes, only a small number of bacteria could adhere to the electrode surface following the treatment with *E. faecium.* Consequently, there was only a modest increase in the ΔR_{ct}, approximately 25 % for bare and NIP-modified electrodes. This comparison highlights the ability of the MIP-modified electrodes to detect *E. faecium,* as they exhibited a significantly greater response compared to the NIP-modified and bare electrodes. Fig. 3H shows the SEM image of the MIP after rebinding with *E. faecium.*

3.2. Sensitivity and selectivity for E. faecium

The MIP-based sensor for *E. faecium* was evaluated across 0 to 10^8 CFU/mL. Fig. 4A shows a gradual EIS response increase with *E. faecium* concentration, due to bacteria partially blocking electron transfer and increasing film impedance. In another study in the literature where E. coli O157:H7 was detected with a polypyrrole-based MIP sensor, similar to our study, the impedance values gradually increase as the bacterial concentration increases due to the partial blocking of the electrode surface by the bacteria [27]. The inset in Fig. 4A shows a linear ΔR_{ct} behavior with bacteria concentration, representing the difference between MIP with and without bacteria. The relationship between bacteria concentration and ΔR_{ct} is given in Eq. (2).

$$\Delta R_{ct} = 22.956 \times \log C - 50.722 \quad (2)$$

where C is the concentration of *E. faecium* in CFU/mL. Based on the calibration study in Fig. 4A-inset, the limit of detection (LOD) and limit of quantification (LOQ) of the biosensor were determined as 9 CFU/mL and 27 CFU/mL, respectively. LOD was calculated using the formula $3 \times SD\sqrt{s}$, and LOQ was calculated using the formula $10 \times SD\sqrt{s}$, where *SD* represents the standard deviation calculated through the regression analysis for the signal-to-noise ratio (S/N) of 3, and *s* is slope of the calibration curve. The LOD value obtained with our developed MIP-based electrochemical biosensor is consistent and competitive with other MIP-based electrochemical biosensors developed for bacterial detection in the literature. In Table 1, we compared our results with the existing literature in terms of bacteria type, electrode type, polymer

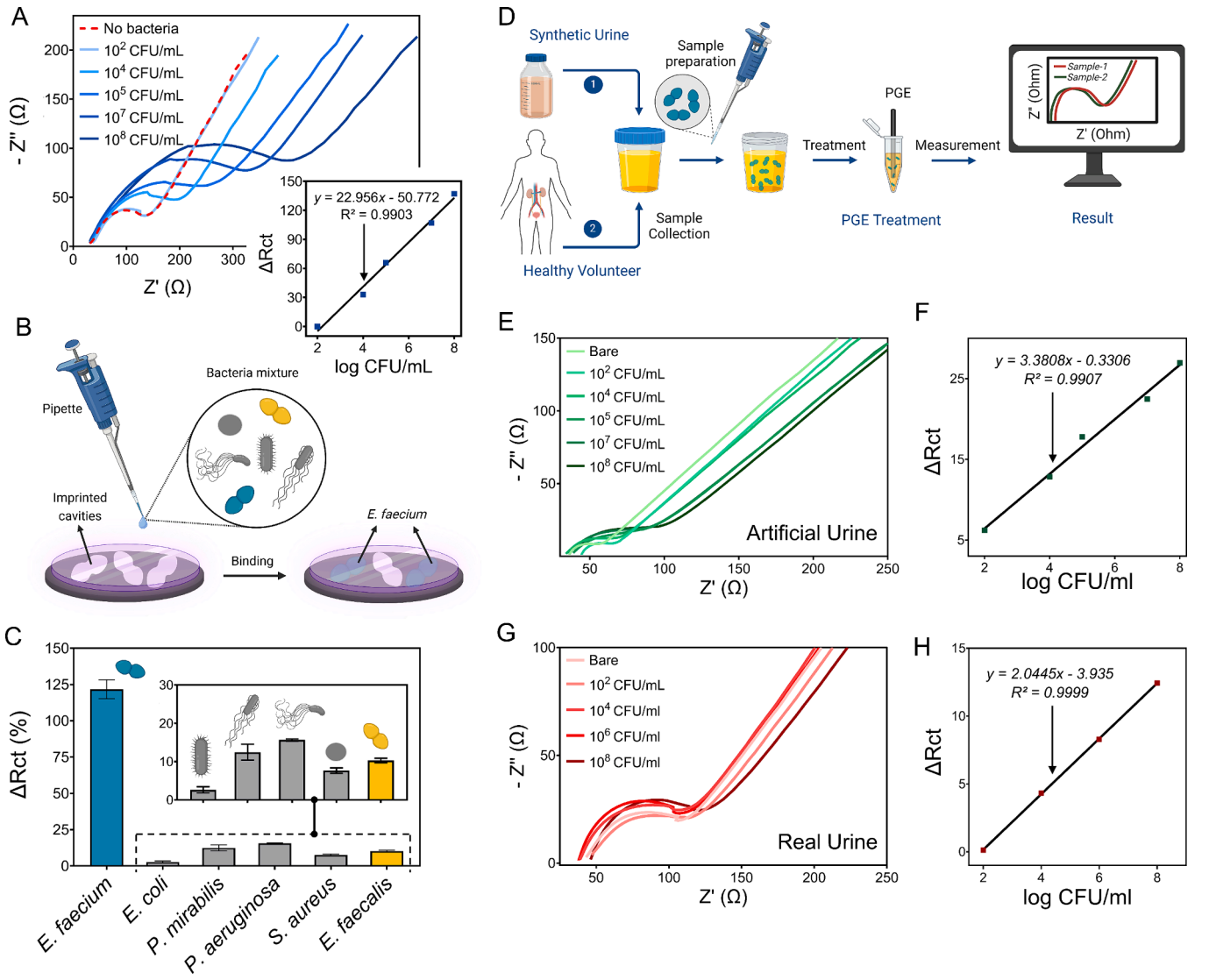

Fig. 4. **(A)** EIS response of the bare (red) and the modified electrodes with *E. faecium* (blue curves) for different concentrations, e.g., 10^2–10^8 CFU/Ml. Figure inset shows the calibration curve containing ΔR_{ct} vs. **(B)** Schematic illustration of the selectivity experiments. **(C)** Percentage change in ΔR_{ct} of the MIP modified electrodes incubated with *E. faecium*. ΔR_{ct} was calculated by comparing the EIS response of the bacteria mixture with PBS. **(D)** Schematic illustration of the detection *E. faecium* from artificial and real urine samples. **(E)** EIS response and **(F)** Calibration plot of bare and 10^2–10^8 CFU/ml *E. faecium* modified electrodes in artificial urine. **(G)** EIS response of bare and 10^2-10^8 CFU/ml *E. faecium* modified electrodes which is in real urine. **(H)** Calibration plot measured with EIS for concentration ranges from 10^2 to 10^8 CFU/mL of *E. faecium* in real urine sample.

composition, removal agent, and sensing technique as well as system LOD or the linear range of bacterial detection.

In addition, we compared the LOD value obtained with the MIP-based biosensor we developed for the detection of *E. faecium* with the LOD values obtained by other methods developed for the detection of this bacterium in the literature. The LOD value obtained with the electrochemical method we developed is quite competitive compared to those obtained by other methods. Table 2 shows other methods developed for the detection of *E. faecium* and the LOD values obtained.

We assessed our MIP-based biosensor's selectivity against various common bacteria causing urinary tract infections. Among the tested bacteria, *Proteus mirabilis, Escherichia coli,* and *Pseudomonas aeruginosa* are Gram-negative bacteria with slight structural differences compared to *E. faecium.* Additionally, *Staphylococcus aureus* is a Gram-positive bacterium with a similar cocci structure to *E. faecium. Enterococcus faecalis* is also a Gram-positive bacterium belonging to the *Enterococcus* genus, closely resembling *E. faecium*. Fig. 4B shows the schematic illustration of the selectivity experiments. In the selectivity experiments, all bacteria were prepared at the same concentration, e.g., 10^5 CFU/mL. After forming the MIP structure on the electrode surface, the sensor was exposed to a mixture of the bacterial species, including the target bacteria. Fig. 4C shows $\%\Delta R_{ct}$ that was calculated by comparing the EIS response of the bacteria mixture with PBS, where the measurements were conducted in 10 mM $K_3/_4[Fe(CN)_6]$ solution. The signal difference for *E. faecium* is significantly larger than for other species, demonstrating the biosensor's high selectivity. It differentiates *E. faecium* from a bacterial mixture, even among structurally similar bacteria, due to imprinted sites with complementary characteristics to the template bacteria. For the study in which bisphenol A was detected using molecularly imprinted polypyrrole, the selectivity of the sensor to the target analyte was determined by using phenolic structures structurally like bisphenol A. Similar to our study, the responses of the polypyrrole-based MIP sensor to structures very similar to the target analyte were very low compared to the target analyte. This shows that high selectivity can be achieved when polypyrrole is used in MIP design and a good sensor design is provided with appropriate removal agents [42].

Table 1
The detection of different bacteria using various MIP-based sensors.

Bacteria	Electrode Type	Polymer	Removing Agent	Method	LOD	Reference
Acinetobacter baumannii	Glassy Carbon Electrode	Polydopamine	0.01 M SDS and 10 mM HNO_3	EIS	30 CFU/mL	[28]
Bacillus cereus spore	Carbon Paste Electrode	Polypyrrole	CTAB	CV	10^2 CFU/mL	[29]
Escherichia coli O157:H7	Glassy Carbon Electrode	Polydopamine	Acetic acid/SDS	Electrochemi-luminescence	8 CFU/mL	[30]
Escherichia coli O157:H7 *Staphylococcus aureus*	Glassy Carbon Electrode	Poly(*o*-phenylenediamine)	CTAB/HAc solution	EIS	9.4 and 9.5 CFU/mL	[31]
Klebsiella pneumonia	ITO-coated Glass Electrode	Polypyrrole	DI and ethanol	DPV and CV	1.352 CFU/mL	[25]
Lactobacillus salivarius	Glassy Carbon Electrode	Polydopamine	Lysozyme under static conditions	Electrochemiluminescence	10^1 – 10^7 CFU/mL	[32]
Listeria monocytogenes	Screen-Printed Carbon Electrode	Polypyrrole	Proteolytic enzyme trypsin	Pulsed Amperometric	70 CFU/mL	[33]
Listeria monocytogenes	Glassy Carbon Electrode	PolyTPA	SDS/AA (w/v, 5 %)	DPV	6 CFU/mL	[34]
Salmonella typhimurium	Au Screen Printed Electrode	Polydopamine	1 % Triton followed by washing with PBS	CV	47 CFU/mL	[35]
Staphylococcus aureus	Gold Electrode	Poly(3-thiopheneacetic acid)	SDS/HAc (5 %, w/v)	EIS	2 CFU/mL	[36]
Staphylococcus epidermidis	Au Disk Electrodes	Poly(3-aminophenylboronic acid (3-APBA))	Fructose solution and deionized water	EIS	10^3–10^7 CFU/mL	[37]
Enterococcus faecium	Pencil Graphite Electrodes	Polypyrrole	SDS/AA (10 %, w/v)	CV, EIS	9 CFU/mL	Our study

*SDS: Sodium dodecyl sulfate, CTAB: Cetyltrimethylammonium bromide, Hac and AA: Acetic acid, DI: Distilled, CFU: Colony-forming unit, DPV: Differential pulse voltammetry, CV: Cyclic voltammetry, EIS: Electrochemical impedance spectroscopy, LOD: Limit of detection.

Table 2
The detection of *E. faecium* with other techniques and obtained LOD values.

Sensing Technique	LOD	Reference
Flow Cytometry combined with Fluorescent Peptide Label	3×10^3 CFU/mL	[38]
Fluorescent *in situ* Hybridization with specific DNA probes	1.1×10^{10} cells (g wet weight)	[39]
Real Time PCR	4.5 CFU/100 mL	[40]
Recombinase Polymerase Amplification-Lateral Flow Strip	1 CFU/μL	[41]
MIP based Electrochemical Impedance Biosensor	9 CFU/mL	This study

3.3. Real sample application

In this section, we demonstrated the capability of our biosensor to selectively identify *E. faecium* with the use of artificial urine with a pH of 5.1 and real urine sample. As schematically illustrated in Fig. 4D, E. *faecium* was introduced into the urine samples at different concentrations ranging from 10^2 to 10^8 CFU/mL. Fig. 4E shows the EIS spectra for different bacteria concentration in artificial urine sample, demonstrating that ΔR_{ct} increased with bacteria concentration. Fig. 4F shows the linear correlation between the percentage change in R_{ct}, ΔR_{ct} (%), response between 10^2 and 10^8 CFU/mL for *E. faecium* samples prepared in artificial urine, similar to the bacterial samples prepared in PBS. Furthermore, the LOD was determined to be approximately 9 CFU/mL in artificial urine samples. These results demonstrate that the developed MIP-based biosensor enables accurate and sensitive analysis in real samples. The impedance responses of the MIP-based biosensor were compared on different days using the same concentration of bacteria with the same synthetic urine and sensor design. The relative standard deviation % (RSD%), which indicates the repeatability of the developed biosensor, was found to be 11.14 %. This result demonstrates that the developed biosensor has good precision.

To demonstrate the practicality of our biosensing methodology, we detected *E. faecium* in real urine samples. The bacteria samples were prepared in untreated real urine across a concentration range of 10^2–10^8 CFU/mL. Fig. 4G shows the EIS spectra for different bacteria concentrations, with ΔRct increasing as bacteria concentration increased. Fig. 4H illustrates the linear correlation between ΔRct (%) and *E. faecium* concentration. The system LOD was calculated as 1.4 CFU/mL for detecting *E. faecium* in real urine samples.

4. Conclusion

In this study, we developed a novel biosensor based on *E. faecium* imprinted polypyrrole for label-free, highly sensitive, and selective detection of *E. faecium*. Surface modification with polypyrrole significantly increased surface area and conductivity compared to bare electrodes, enabling more sensitive detection. *E. faecium* imprinted polypyrrole (MIP) was synthesized directly on the electrode via electropolymerization. Non-imprinted polypyrrole (NIP) was synthesized without *E. faecium* template as a control. Specific cavities formed on the MIP surface, treated with 10 % acetic acid and 10 % SDS, served as a key-lock mechanism for detecting *E. faecium*. The biosensor demonstrated high selectivity, with negligible response to *Proteus mirabilis, Escherichia coli,* and *Pseudomonas aeruginosa*. It exhibited linearity between 10^2 and 10^8 CFU/mL, with a detection limit of 9 CFU/mL. The biosensor successfully detected *E. faecium* in both artificial and real urine samples. With applications such as the integration of nanomaterials and screen-printed electrodes into the developed MIP-based biosensor structure, a more sensitive and portable alternative point-of-care testing method could be obtained. Especially by reducing the bacterial detection time from one or two days to a few hours, the method demonstrates that it could serve as an alternative for early detection of infections caused by this bacterium and/or other bacteria when the method is translated to a lab-on-a-chip application with further studies. In this way, portable tests that enable accurate, early, and selective bacterial detection can facilitate the prompt and optimal treatment of infections and prevent susceptibility issues that could arise from incorrect antibiotic use.

CRediT authorship contribution statement

Hüseyin Oğuzhan Kaya: Writing – review & editing, Writing – original draft, Visualization, Validation, Methodology, Investigation, Formal analysis, Data curation, Conceptualization. **Yamaç Tekintaş:** Writing – original draft, Validation, Methodology, Investigation, Formal analysis, Data curation. **Fatma Kurul:** Writing – original draft,

Visualization, Validation. **Arif E. Cetin:** Writing – original draft, Visualization, Project administration, Methodology. **Seda Nur Topkaya:** Writing – review & editing, Writing – original draft, Visualization, Validation, Supervision, Resources, Methodology, Investigation, Funding acquisition, Formal analysis, Data curation, Conceptualization.

Declaration of competing interest

The authors declare that they have no known competing financial interests or personal relationships that could have appeared to influence the work reported in this paper.

Acknowledgment

This study has been supported by the grant of Izmir Katip Celebi University Scientific Research Projects Coordination Unit, Project No: 2022-GAP-ECZF-0009.

References

[1] X. Zhou, R.J.L. Willems, A.W. Friedrich, J.W.A. Rossen, E. Bathoorn, *Enterococcus faecium*: from microbiological insights to practical recommendations for infection control and diagnostics, Antimicrob. Resist. Infect. Control 9 (1) (2020) 130.
[2] S. Jain, A. Kumar, B. Kashyap, I.R. Kaur, Clinico-epidemiological profile and high-level aminoglycoside resistance in *Enterococcal septicemia* from a tertiary care hospital in east Delhi, Int. J. Appl. Basic Med. Res. 1 (2) (2011) 80–83.
[3] C. Johnson, C. Marquez, D. Olson, T. Ward, S. Cheney, T. Hulten, T. Ton, C. R. Webb, J. Dunn, Development and performance of a multiplex PCR assay for the detection of bacteria in sterile body fluids, Fut. Microbiol. 18 (2023) 187–195.
[4] C.M. Brown, C. Staley, P. Wang, B. Dalzell, C.L. Chun, M.J. Sadowsky, A high-throughput DNA-sequencing approach for determining sources of fecal bacteria in a lake superior estuary, Environ. Sci. Technol. 51 (15) (2017) 8263–8271.
[5] H. Schmidt, S. Gorka, D. Seki, A. Schintlmeister, D. Woebken, Gold-FISH enables targeted NanoSIMS analysis of plant-associated bacteria, New Phytol. 240 (1) (2023) 439–451.
[6] M. Smolejova, J. Krcmarikova, I. Cihova, P. Sulo, Are ELISA and PCR Discrepancies in the Identification of Chlamydia pneumoniae Caused by the Presence of "Chlamydia-Related Bacteria"? Microorganisms 11 (1) (2023).
[7] J. Sevestre, M.A.O. Lemrabott, J.M. Berenger, A. Zan Diarra, A. Ould Mohamed Salem Boukhary, P. Parola, Detection of Arthropod-Borne Bacteria and Assessment of MALDI-TOF MS for the Identification of Field-Collected Immature Bed Bugs from Mauritania, Insects 14 (1) (2023).
[8] Y. Chang, K. Jiang, L. Zhang, F. Yang, J. Huang, Application of next-generation sequencing technology in the detection of pathogenic bacteria of the periprosthetic joint infection after arthroplasty, Int Wound J 20 (6) (2023) 2121–2128.
[9] N. Idil, B. Mattiasson, Imprinting of Microorganisms for Biosensor Applications, Sensors (Basel) 17 (4) (2017).
[10] R. Zhu, X. Wang, J. Ma, Q. Jia, Preparation of poly(caffeic acid)-coated epitope molecularly imprinted polymers and investigation of adsorption performance toward ovalbumin, J. Chromatogr. A 1716 (2024) 464635.
[11] A.T. Cardoso, R.O. Martins, F.M. Lancas, A.R. Chaves, Molecularly imprinted polymers in online extraction liquid chromatography methods: Current advances and recent applications, Anal. Chim. Acta 1284 (2023) 341952.
[12] A. Garcia-Cruz, O.S. Ahmad, K. Alanazi, E. Piletska, S.A. Piletsky, Generic sensor platform based on electro-responsive molecularly imprinted polymer nanoparticles (e-NanoMIPs), Microsyst. Nanoeng. 6 (1) (2020) 83.
[13] M. Garg, N. Pamme, Strategies to remove templates from molecularly imprinted polymer (MIP) for biosensors, TrAC Trends Anal. Chem. 170 (2024) 117437.
[14] A. Ramanavicius, A. Finkelsteinas, H. Cesiulis, A. Ramanaviciene, Electrochemical impedance spectroscopy of polypyrrole based electrochemical immunosensor, Bioelectrochemistry 79 (1) (2010) 11–16.
[15] S. Ramanavicius, A. Ramanavicius, Development of molecularly imprinted polymer based phase boundaries for sensors design (review), Adv. Colloid Interface Sci. 305 (2022) 102693.
[16] Y.L. Mustafa, A. Keirouz, H.S. Leese, Molecularly imprinted polymers in diagnostics: accessing analytes in biofluids, J. Mater. Chem. B 10 (37) (2022) 7418–7449.
[17] J. Wu, R. Wang, Y. Lu, M. Jia, J. Yan, X. Bian, Facile Preparation of a Bacteria Imprinted Artificial Receptor for Highly Selective Bacterial Recognition and Label-Free Impedimetric Detection, 91(1) (2019) 1027-1033.
[18] T. Kilic, Y.K. Cho, N. Jeong, I.S. Shin, Multielectrode Spectroscopy Enables Rapid and Sensitive Molecular Profiling of Extracellular Vesicles, 8(1) (2022) 110-117.
[19] Y. Ma, X.L. Shen, Q. Zeng, H.S. Wang, L.S. Wang, A multi-walled carbon nanotubes based molecularly imprinted polymers electrochemical sensor for the sensitive determination of HIV-p24, Talanta 164 (2017) 121–127.
[20] A. Ben Hassine, N. Raouafi, F.T.C. Moreira, Novel Electrochemical Molecularly Imprinted Polymer-Based Biosensor for Tau Protein Detection, Chemosensors 9 (9) (2021) 238.
[21] K. Ramajayam, S. Ganesan, P. Ramesh, M. Beena, T. Kokulnathan, A. Palaniappan, Molecularly imprinted polymer-based biomimetic systems for sensing environmental contaminants, biomarkers, and bioimaging applications, Biomimetics (Basel) 8 (2) (2023).
[22] R. Jain, N. Jadon, A. Pawaiya, Polypyrrole based next generation electrochemical sensors and biosensors: A review, TrAC Trends Anal. Chem. 97 (2017) 363–373.
[23] T. Kilic, Y.K. Cho, N. Jeong, I.-S. Shin, B.S. Carter, L. Balaj, R. Weissleder, H. Lee, Multielectrode spectroscopy enables rapid and sensitive molecular profiling of extracellular vesicles, ACS Cent. Sci. 8 (1) (2022) 110–117.
[24] M. Tefera, M. Tessema, S. Admassie, M. Ward, L. Phelane, E.I. Iwuoha, P.G. L. Baker, Electrochemical application of cobalt nanoparticles-polypyrrole composite modified electrode for the determination of phoxim, Anal. Chim. Acta: X 9 (2021) 100077.
[25] R. Sharma, G.B.V.S. Lakshmi, A. Kumar, P. Solanki, Polypyrrole Based Molecularly Imprinted Polymer Platform for Klebsiella pneumonia Detection, ECS Sensors Plus 1 (1) (2022) 010603.
[26] G. Bolat, Y.T. Yaman, S. Abaci, Molecularly imprinted electrochemical impedance sensor for sensitive dibutyl phthalate (DBP) determination, Sensors Actuat. B: Chem. (2019).
[27] J. Wu, R. Wang, Y. Lu, M. Jia, J. Yan, X. Bian, Facile Preparation of a Bacteria Imprinted Artificial Receptor for Highly Selective Bacterial Recognition and Label-Free Impedimetric Detection, Anal. Chem. 91 (1) (2019) 1027–1033.
[28] M. Roushani, M. Sarabaegi, A. Rostamzad, Novel electrochemical sensor based on polydopamine molecularly imprinted polymer for sensitive and selective detection of Acinetobacter baumannii, J. Iran. Chem. Soc. 17 (9) (2020) 2407–2413.
[29] A. Ait Lahcen, F. Arduini, F. Lista, A. Amine, Label-free electrochemical sensor based on spore-imprinted polymer for Bacillus cereus spore detection, Sens. Actuators B 276 (2018) 114–120.
[30] S. Chen, X. Chen, L. Zhang, J. Gao, Q. Ma, Electrochemiluminescence Detection of Escherichia coli O157:H7 Based on a Novel Polydopamine Surface Imprinted Polymer Biosensor, ACS Appl. Mater. Interfaces 9 (6) (2017) 5430–5436.
[31] X. Xu, X. Lin, L. Wang, Y. Ma, T. Sun, X. Bian, A Novel Dual Bacteria-Imprinted Polymer Sensor for Highly Selective and Rapid Detection of Pathogenic Bacteria, Biosensors 13 (9) (2023) 868.
[32] L. Wang, Y. Nie, P. Wang, Y. Li, Q. Ma, D. Yu, A novel bacterial imprinted polymers- electrochemiluminescent sensor for Lactobacillus salivarius detection, Sens. Actuators B 358 (2022) 131467.
[33] V. Liustrovaite, M. Pogorielov, R. Boguzaite, V. Ratautaite, A. Ramanaviciene, G. Pilvenyte, V. Holubnycha, V. Korniienko, K. Diedkova, R. Viter, A. Ramanavicius, Towards Electrochemical Sensor Based on Molecularly Imprinted Polypyrrole for the Detection of Bacteria—Listeria monocytogenes, Polymers 15 (7) (2023) 1597.
[34] Q. Li, Z. Guo, X. Qiu, W. Lu, W. Yang, Q. Wang, Q. Wu, Simple electrochemical detection of Listeria monocytogenes based on a surface-imprinted polymer-modified electrode, Anal. Methods 13 (41) (2021) 4864–4870.
[35] S.A. Khalid, R.Y.A. Hassan, R.M. El Nashar, I.M. El-Sherbiny, Voltammetric determination of Salmonella typhimurium in minced beef meat using a chip-based imprinted sensor, RSC Adv. 12 (6) (2022) 3445–3453.
[36] R. Wang, L. Wang, J. Yan, D. Luan, S. Tao, J. Wu, X. Bian, Rapid, sensitive and label-free detection of pathogenic bacteria using a bacteria-imprinted conducting polymer film-based electrochemical sensor, Talanta 226 (2021) 122135.
[37] M. Golabi, F. Kuralay, E.W.H. Jager, V. Beni, A.P.F. Turner, Electrochemical bacterial detection using poly(3-aminophenylboronic acid)-based imprinted polymer, Biosens. Bioelectron. 93 (2017) 87–93.
[38] T.F. Oftedal, D.B. Diep, Flow cytometric detection of vancomycin-resistant Enterococcus faecium in urine using fluorescently labelled enterocin K1, Sci. Rep. 13 (1) (2023) 10930.
[39] K. Waar, J.E. Degener, M.J. van Luyn, H.J. Harmsen, Fluorescent in situ hybridization with specific DNA probes offers adequate detection of Enterococcus faecalis and Enterococcus faecium in clinical samples, J. Med. Microbiol. 54 (10) (2005) 937–944.
[40] A.F. Maheux, L. Bissonnette, M. Boissinot, J.-L.-T. Bernier, V. Huppé, È. Bérubé, D. K. Boudreau, F.J. Picard, A. Huletsky, M.G. Bergeron, Method for rapid and sensitive detection of Enterococcus sp. and Enterococcus faecalis/faecium cells in potable water samples, Water Res. 45 (6) (2011) 2342–2354.
[41] L. Wang, T. Zhang, J. Huo, Y. Wang, Y. Lu, X. Zhu, Rapid and specific detection of Enterococcus faecium with an isothermal amplification and lateral flow strip combined method, Arch. Microbiol. 206 (1) (2023) 28.
[42] F. Tan, L. Cong, X. Li, Q. Zhao, H. Zhao, X. Quan, J. Chen, An electrochemical sensor based on molecularly imprinted polypyrrole/graphene quantum dots composite for detection of bisphenol A in water samples, Sens. Actuators B 233 (2016) 599–606.